

On Robustness against Measurement Noise of Iterative Learning Control based Identification

Toshiharu Sugie* Fumitoshi Sakai**

* *Department of Systems Science, Kyoto University, Uji, Kyoto
611-0011, Japan, (e-mail: sugie@i.kyoto-u.ac.jp)*

** *Department of Mechanical Engineering, Nara National College of
Technology, Yamatokoriyama, Nara 639-1080, Japan, (e-mail:
sakai@mech.nara-k.ac.jp)*

Abstract: One of the most important issues in control system design is to obtain an accurate model of the plant to be controlled. Though most of the existing identification methods are described in discrete-time, it would be more appropriate to have continuous-time models directly from the sampled I/O data. From this viewpoint, the authors have developed such a direct identification method based on ILC (Iterative Learning Control) approach. This is a new application area of ILC. The method often yields accurate models even in the presence of heavy measurement noise. The robustness against noise is achieved through (i) projection of continuous-time I/O signals onto a finite dimensional parameter space, (ii) initial models through preparatory experiment and (iii) noise tolerant learning laws. This paper examines the accuracy of the initial models and convergence property of ILC in the presence of heavy colored noise through detailed simulations, which demonstrates the robustness of the ILC based identification method.

Keywords: identification, linear systems, continuous-time systems, learning control, stochastic systems

1. INTRODUCTION

One of the most important issues in control system design is to obtain an accurate model of the plant to be controlled. Though most of the existing identification methods are described in discrete-time, it would be convenient to have continuous-time models directly from the I/O data. In fact, it is often easier for us to capture the plant dynamics intuitively in continuous-time rather than in discrete-time. So far a lot of researchers try to obtain the continuous-time models directly (namely, without recourse to the discrete-time models) from the I/O data. Comprehensive surveys on this topic have been given by Young [1981], Unbehauen and Rao [1990] and Sinha and Rao [1991]. Furthermore, the CONTinuous-Time System IDENTification (CONTSID) tool-box has been developed on the basis of these direct methods [Garnier and Mensler, 1999, 2000, Garnier et al., 2003]. A basic difficulty is that standard approaches require the time-derivatives of I/O data in the presence of measurement noise.

On the other hand, iterative learning control (ILC) has attracted much attention over the last two decades as a powerful model-free control methodology [Arimoto et al., 1984, Kawamura et al., 1988, Moore, 1993, Bein and Xu, 1998, Chen and Wen, 1999]. ILC yields the input which achieves perfect output tracking by iteration of trials for uncertain systems. Though ILC can deal with plants having large uncertainty, most ILC approaches need time-derivatives of I/O data in the continuous-time case

[Sugie and Ono, 1991], and therefore it is quite sensitive to measurement noise. Recently, Hamamoto and Sugie [2001, 2002] proposed an ILC where the learning law works in a certain finite-dimensional subspace and showed that any time-derivative of the tracking error is not required to achieve perfect tracking in their scheme. Based on this work, Sugie and Sakai [2005] and Sakai and Sugie [2006], proposed an ILC which works in the presence of heavy measurement noise, and, moreover, the method was shown to be applicable to the identification of continuous-time systems as well. This identification method has several advantages such as: (i) no time-derivatives of I/O data are required, (ii) it gives unbiased estimations. This work was followed by Campi et al. [2006]. They show a way how to deal with plant zeros and provide more noise tolerant learning laws which guarantee zero convergence of the parameter estimation errors as the number of trials increases. Further, Sakai and Sugie [2007] extend this result to the closed loop system identification.

The purpose of this paper is to evaluate the robustness of this type of ILC based identification method against the heavy measurement noise through simulation study. In particular, (a) the accuracy of the initial models obtained through the preliminary experiments and (b) convergence of iterative learning against errors in initial models are examined subject to colored measurement noise extensively.

The following notations will be used. Superscript denotes the trial number and subscript denotes the element of a

set or a matrix. For instance, input u at the k -th trial is written as u^k while x_i is the i -th element of the vector x .

2. SYSTEM DESCRIPTION

Consider the continuous-time SISO system described by

$$y(t) = \frac{B^\circ(p)}{A^\circ(p)} u(t) \triangleq \frac{1 + \beta_1^\circ p + \dots + \beta_m^\circ p^m}{\alpha_0^\circ + \alpha_1^\circ p + \dots + \alpha_n^\circ p^n} u(t) \quad (1)$$

where $u(t)$ and $y(t)$, $t \in [0, T]$, are the input and the output, respectively, $\alpha_i^\circ \in \mathbb{R}$ ($i = 0, 1, \dots, n$) and $\beta_i^\circ \in \mathbb{R}$ ($i = 1, \dots, m$) are coefficient parameters, while p is the differential operator, *i.e.*, $pu(t) = du(t)/dt$. We assume the following:

- Many experiments on the system can be repeated with zero initial state on the time interval $[0, T]$.
- Though the true parameters α_i° and β_i° are unknown, $A^\circ(p)$ and $B^\circ(p)$ are coprime and their order n and m are known.
- We can measure $\tilde{y}(t)$, the output contaminated with noise,

$$\tilde{y}(t) = y(t) + w(t)$$

where $w(t)$ is zero-mean measurement noise.

The goal is to determine a model in the class

$$\mathcal{M} = \left\{ \frac{B(p)}{A(p)} = \frac{1 + \beta_1 p + \dots + \beta_m p^m}{\alpha_0 + \alpha_1 p + \dots + \alpha_n p^n} \right\}$$

based on I/O measurements $u(t)$ and $\tilde{y}(t)$.

3. IDENTIFICATION PROCEDURE

This section describes a basic idea of how to identify the system through iteration of trials. For conceptual simplicity, we discuss the case where the system has no finite zeros, *i.e.*, $B^\circ(p) = 1$ in this section. The general case will be discussed later.

3.1 Iterative identification scheme via projection

First, choose a smooth signal $r(t)$, $t \in [0, T]$ satisfying

$$r(0) = 0, \quad \dot{r}(0) = 0, \quad \dots, \quad r^{(n-1)}(0) = 0.$$

At the k -th trial, perform the following experiment on $[0, T]$ which produces the signal $\varepsilon^k(t)$ when the parameter estimates $\alpha_0^k, \dots, \alpha_n^k$ are given.

- Define $A^k(p) \triangleq \alpha_0^k + \alpha_1^k p + \dots + \alpha_n^k p^n$
- Inject $u^k(t) = A^k(p)r(t)$ into the system.
- Observe the corresponding output $\tilde{y}^k(t)$.
- Compute the tracking error signal $\varepsilon^k(t)$ by

$$\varepsilon^k(t) = \tilde{y}^k(t) - r(t).$$

Note that $\varepsilon^k(t)$ is obtained without taking any derivative of noisy measurements, only derivatives of $r(t)$ are required. Note also that $\varepsilon^k(t)$ can also be written as

$$\varepsilon^k(t) = \frac{A^k(p) - A^\circ(p)}{A^\circ(p)} r(t) + w^k(t). \quad (2)$$

Now, we introduce the finite-dimensional subspace described by

$$\mathcal{F} \triangleq \text{span}\{f_1(t), f_2(t), \dots, f_{n+1}(t)\}$$

where $\{f_1(t), \dots, f_{n+1}(t)\}$ is an appropriate basis chosen by the designer. Then project $\varepsilon^k(t)$ onto \mathcal{F} . The projection is written as

$$\varepsilon^k(t)|_{\mathcal{F}} = \delta_1^k f_1(t) + \dots + \delta_{n+1}^k f_{n+1}(t)$$

and $\delta^k \triangleq [\delta_1^k, \dots, \delta_{n+1}^k]^T$ is its vector representation. Let for brevity

$$\gamma^\circ = [\alpha_0^\circ, \alpha_1^\circ, \dots, \alpha_n^\circ]^T, \quad \gamma^k = [\alpha_0^k, \alpha_1^k, \dots, \alpha_n^k]^T,$$

then the iterative identification procedure is described as follows:

(Step 0) Given γ^0 , set $k = 0$.

(Step 1) Generate δ^k from γ^k .

(Step 2) Update γ^k by

$$\gamma^{k+1} = \gamma^k + H^k \delta^k, \quad (3)$$

where $H^k \in \mathbb{R}^{(n+1) \times (n+1)}$ is the learning gain. If the designer satisfies the model accuracy, stop the iteration. Otherwise, set $k = k + 1$ and go to Step 1.

3.2 Update law

The choice of H^k is discussed in this subsection.

Suppose, for the time being, $w^k(t) = 0$ holds. It is easy to see that the tracking error $\delta^k \in \mathbb{R}^{n+1}$ depends on the parameter estimate $\gamma^k \in \mathbb{R}^{n+1}$ linearly. So there exist a matrix $M \in \mathbb{R}^{(n+1) \times (n+1)}$ and an offset term $\bar{\delta} \in \mathbb{R}^{n+1}$ such that

$$\delta^k = M\gamma^k + \bar{\delta} \quad (4)$$

holds. Suppose that $f_i(t)$'s are chosen so that M is non-singular. Due to $w^k(t) = 0$, $\gamma^k = \gamma^\circ$ implies $\delta^k = 0$ from (2). Therefore, $\bar{\delta} = -M\gamma^\circ$ must hold. Thus, (4) can be re-written as

$$\delta^k = M(\gamma^k - \gamma^\circ)$$

with M non-singular. When noise $w^k(t)$ is taken into account, δ^k becomes

$$\delta^k = M(\gamma^k - \gamma^\circ) + \nu^k \quad (5)$$

where ν^k accounts for the projection of $w^k(t)$ onto \mathcal{F} . This is the basic equation to determine the learning gain.

Eqns. (5) and (3) yields

$$\gamma^{k+1} = \gamma^k + H^k M(\gamma^k - \gamma^\circ) + H^k \nu^k$$

Thus, defining $\tilde{\gamma}^k \triangleq \gamma^k - \gamma^\circ$ we have

$$\tilde{\gamma}^{k+1} = (I + H^k M)\tilde{\gamma}^k + H^k \nu^k \quad (6)$$

which describes how the error $\tilde{\gamma}^k$ propagates through trials. Now, let

$$\Phi \triangleq \mathbf{E}[\nu^k (\nu^k)^T], \quad P^k \triangleq \mathbf{E}[\tilde{\gamma}^k (\tilde{\gamma}^k)^T],$$

and show how to select H^k so as to reduce P^k optimally under the assumption that M and Φ are known. Noise is assumed to be independent in different experiments. From (6), we have:

$$P^{k+1} = (I + H^k M)P^k(I + H^k M)^T + H^k \Phi (H^k)^T$$

Therefore, P^{k+1} is minimized by the choice

$$H^k = -P^k M^T (M P^k M^T + \Phi)^{-1} \quad (7)$$

With this choice, we obtain

$$P^{k+1} = P^k - P^k M^T (M P^k M^T + \Phi)^{-1} M P^k \quad (8)$$

Eqns. (7) and (8), where (8) is initialized with

$$P^0 = \mathbf{E}[\tilde{\gamma}^0 (\tilde{\gamma}^0)^T]. \quad (9)$$

Based on the above idea, the following result has been obtained.

Theorem 1:[Campi et al., 2006] Suppose we adopt the updating law (3) with (7), (8) and (9). Then it holds that

$$\mathbf{E}[(\gamma^k - \gamma^\circ)(\gamma^k - \gamma^\circ)^T] \rightarrow 0, \text{ as } k \rightarrow \infty. \quad (10)$$

It implies that the method gives us the true parameter γ° in the presence of measurement noise through iteration of trials. Further, an alternative version is given as follows.

Theorem 2:[Campi et al., 2006] If the updating law (3) is adopted where H^k is given by

$$H^k = -\frac{1}{k+1}M^{-1}, \quad (11)$$

then (10) holds. \square

4. DIGITAL IMPLEMENTATION

Now we discuss how to implement the iterative identification method when the I/O data are available only at the sampled times. Namely, we suppose that the I/O data are $\{u(iT_s), \tilde{y}(iT_s)\}$ ($i = 0, 1, \dots, q$), where T_s is sampling time satisfying $qT_s = T$, and the input is injected to the plant via the zero-order holder (ZOH).

4.1 Representation in the projected space

Suppose that the reference signal $r(t)$ is chosen. Define

$$V_r(t) = \left[r(t), \frac{dr(t)}{dt}, \dots, \frac{d^n r(t)}{dt^n} \right],$$

then, we have

$$u(t)^k = A^k(p)r(t) = V_r(t)\gamma^k.$$

Since the data are available only at sampled times, we define

$$\mathbf{u}^k \triangleq [u^k(0), u^k(T_s), \dots, u^k(qT_s)]^T \in \mathbb{R}^{q+1}$$

$$\tilde{\mathbf{y}}^k \triangleq [\tilde{y}^k(0), \tilde{y}^k(T_s), \dots, \tilde{y}^k(qT_s)]^T \in \mathbb{R}^{q+1}.$$

The vectors $\mathbf{r}^k \in \mathbb{R}^{q+1}$, $\mathbf{y}^k \in \mathbb{R}^{q+1}$, $\boldsymbol{\varepsilon}^k \in \mathbb{R}^{q+1}$ and $\mathbf{w}^k \in \mathbb{R}^{q+1}$ are defined in the same way. Similarly, let $V_{dr} \in \mathbb{R}^{(q+1) \times (n+1)}$ be

$$V_{dr} \triangleq \begin{bmatrix} r(0) & \dot{r}(0) & \dots & r^{(n)}(0) \\ r(T_s) & \dot{r}(T_s) & \dots & r^{(n)}(T_s) \\ \vdots & \vdots & \dots & \vdots \\ r(qT_s) & \dot{r}(qT_s) & \dots & r^{(n)}(qT_s) \end{bmatrix}.$$

Then, we have

$$\mathbf{u}^k = V_{dr}\gamma^k. \quad (12)$$

While, let $\{f_1(t), f_2(t), \dots, f_{n+1}(t)\}$ are given functions, and define $V_{df} \in \mathbb{R}^{(q+1) \times (n+1)}$ by

$$V_{df} \triangleq \begin{bmatrix} f_1(0) & f_2(0) & \dots & f_{n+1}(0) \\ f_1(T_s) & f_2(T_s) & \dots & f_{n+1}(T_s) \\ \vdots & \vdots & \dots & \vdots \\ f_1(qT_s) & f_2(qT_s) & \dots & f_{n+1}(qT_s) \end{bmatrix}.$$

Let the QR decomposition of V_{df} be

$$V_{df} = UR, \quad U^T U = I_{n+1},$$

where $U \triangleq [\mathbf{f}_1, \mathbf{f}_2, \dots, \mathbf{f}_{n+1}] \in \mathbb{R}^{(q+1) \times (n+1)}$ and $R \in \mathbb{R}^{(n+1) \times (n+1)}$ is a nonsingular upper triangular matrix. These \mathbf{f}_i 's constitute an orthogonal basis for projection in the digital implementation. Therefore, for example, the vector representation of $\boldsymbol{\varepsilon}^k$ and \mathbf{w}^k are given by

$$\boldsymbol{\delta}^k = U^T \boldsymbol{\varepsilon}^k, \quad \boldsymbol{\nu}^k = U^T \mathbf{w}^k,$$

4.2 Estimate of M

If we inject the input sequence \mathbf{u}^k with the ZOH, the corresponding output \mathbf{y}^k is given by

$$\mathbf{y}^k = G\mathbf{u}^k$$

irrespective of k , where G is specified by

$$G = \begin{bmatrix} g_0 & 0 & 0 & \dots & 0 \\ g_1 & g_0 & 0 & \dots & 0 \\ g_2 & g_1 & g_0 & \dots & 0 \\ \vdots & \vdots & \vdots & \dots & \vdots \\ g_N & g_{N-1} & g_{N-2} & \dots & g_0 \end{bmatrix} \in \mathbb{R}^{(q+1) \times (q+1)}. \quad (13)$$

The first column of G is the output \mathbf{y} when we inject the input $\mathbf{u} = [1, 0, 0, \dots, 0]^T$. The tracking error is obtained by

$$\boldsymbol{\varepsilon}^k = G\mathbf{u}^k + \mathbf{w}^k - \mathbf{r}.$$

Through the projection, we have

$$\boldsymbol{\delta}^k = U^T G V_{dr} (\gamma^k - \gamma^\circ) + \boldsymbol{\nu}^k$$

with the aid of $\mathbf{u}^k = V_{dr}\gamma^k$ and $\mathbf{r} = G V_{dr}\gamma^\circ$. This implies that

$$M = U^T G V_{dr} \quad (14)$$

$$\gamma^\circ = M^{-1} U^T \mathbf{r}. \quad (15)$$

Note that we can obtain an estimate \hat{G} of G through simple experiments. For example, observe the unit step responses twice (with independent measurement noises), say, $\tilde{y}_{step1}(t)$ and $\tilde{y}_{step2}(t)$. Then, we obtain $\hat{g}_0 = 0$ and

$$\hat{g}_i = \tilde{y}_{step1}(iT_s) - \tilde{y}_{step2}((i-1)T_s) \quad \text{for } i \geq 1.$$

Once we have \hat{G} , we obtain an estimate of M by computing $\hat{M} = U^T \hat{G} V_{dr}$.

4.3 Identification steps

The total identification steps are summarized as follows:

- (Step a) Choose the reference signal $r(t)$.
- (Step b) Obtain $\{g_i\}$ in (13) through experiments, and estimate M .
- (Step c) Perform the iterative identification.

If the estimate \hat{M} is so poor, the iterative procedure may not converge. Therefore the quality of \hat{M} is very important. Also, it is useful to know how robust the leaning law against the modeling error in \hat{M} . Therefore, these two points will be evaluated through simulations under heavy measurement noise. In particular, the performance of the proposed method against the colored noise will be studied extensively, because the robustness against the colored noise is one of the distinguished merits of the proposed method.

5. EXTENSION TO GENERAL CASE

So far, we have discussed the case where the system has no finite zeros. This section briefly shows how to extend the identification procedure to the general case [Campi et al., 2006] before proceeding to the simulation stage,

Consider the plant $B^\circ(p)/A^\circ(p)$ described in (1). The procedure is almost the same except we compute the following error signal

$$\begin{aligned} \varepsilon^k(t) &= \tilde{y}^k(t) - B^k(p)r(t) \\ B^k(p) &\triangleq 1 + \beta_1^k p + \dots + \beta_m^k p^m \end{aligned} \quad (16)$$

in stead of $\varepsilon^k(t) = \tilde{y}^k(t) - r(t)$, where $\{\beta_1^k, \dots, \beta_m^k\}$ are the parameter estimates of $\{\beta_1^\circ, \dots, \beta_m^\circ\}$.

Using the projection onto

$$\mathcal{F} \triangleq \text{span}\{f_1(t), f_2(t), \dots, f_{n+m+1}(t)\},$$

we have (5) with

$$\begin{aligned} \gamma^\circ &= [\alpha_0^\circ, \dots, \alpha_n^\circ, \beta_1^\circ, \dots, \beta_m^\circ]^T, \\ \gamma^k &= [\alpha_0^k, \dots, \alpha_n^k, \beta_1^k, \dots, \beta_m^k]^T \end{aligned}$$

Therefore, the update laws given in section 3 can be used.

Concerning to digital implementation, M should be replaced by

$$M = U^T [GV_{dr}, -V_{dr}[2 : m + 1]],$$

according to (16). Here $V_{dr}[2 : m + 1]$ means the matrix $[v_2, v_3, \dots, v_{m+1}]$ where v_i denotes the i -th column of V_{dr} .

6. SIMULATION

Consider the non-minimum phase system described by

$$P(s) = \frac{-T_1 s + 1}{\left(\frac{s^2}{\omega_{n,1}^2} + \frac{2\zeta_1 s}{\omega_{n,1}} + 1\right) \left(\frac{s^2}{\omega_{n,2}^2} + \frac{2\zeta_2 s}{\omega_{n,2}} + 1\right)},$$

where $T_1 = 4$ [s], $\omega_{n,1} = 20$ [rad/s], $\zeta_1 = 0.1$, $\omega_{n,2} = 2$ [rad/s], and $\zeta_2 = 0.25$. The time interval of each trial is $T = 10$ [s] and the sampling period is $T_s = 0.01$ [s].

The signal $r(t)$ is chosen to be the output of the following system

$$F(s) = \frac{1}{(0.1s + 1)^5}$$

when a square wave is injected. We also choose the basis functions as $f_i(t) = r^{(i-1)}(t)$ for $i = 1 \sim 5$.

6.1 Accuracy of \hat{M}

First, we examine the accuracy of the estimate \hat{M} when the measurement data $\{g_i\}$ in (13) are corrupted with colored noise. An example of the data $\{g_i\}$ are shown in Fig.1. The thick line shows the true $\{g_i\}$, which corresponds to the impulse response of the discretized target system, and the dotted line is the measured value subject to the colored noise which is the output of the filter

$$W(s) = \frac{\omega_n^2}{s^2 + 2\zeta\omega_n s + \omega_n^2}$$

with white noise input, $\zeta = 0.1$ and $\omega_n = 25$ [rad/s]. The NSR (noise to signal ratio) is around 50 %. We obtain the data under various NSR and ω_n , then calculate \hat{M} for

each case. In order to evaluate the accuracy, we use the Hankel norm of the error system, i.e., $\|P(s) - \hat{P}(s)\|_H$, where $\hat{P}(s)$ is the estimate of $P(s)$ obtained from \hat{M} . Note that the estimate of the true system parameter γ° can determined from \hat{M} via (15) and that $\|P(s)\|_H = 8.6465$. Fig. 2 shows $\|P(s) - \hat{P}(s)\|_H$ for NSR = 0 ~ 50 % with various colored/white noise. We run the simulation 50 times for each NSR and ω_n , and each line shows the average of 50 runs. From this figure, we can see the following: Even if the noise-free case, the estimation error occurs. As NSR grows, the error becomes bigger, and the effect (or contribution to the modeling error) of white noise is relatively small compared to colored ones. The effect of noise with $\omega_n = 25$ [rad/s] is bigger than the other colored noises. The reason would be that $\omega_n = 25$ [rad/s] is closer to one of the system poles (i.e., $\omega_{n,1} = 20$ [rad/s]) than any others. In this figure, the case of (NSR=50%, $\omega_n = 25$ [rad/s]) looks terrible. However it is not so bad if we take a closer look. Fig. 3 shows $\|P(s) - \hat{P}(s)\|_H$ for each run in this case, which tells us that most of them are good and one (or two) out of 50 runs behaves bad. Therefore, we may say that we can obtain a relatively good model for most cases even if we have heavy colored noise in measurement. Fig. 4 shows the Bode plots of $\hat{P}(s)$ for 50 runs in case of (NSR=50%, $\omega_n = 25$ [rad/s]). The bundle shows 50 plot lines of $\hat{P}(s)$ and the thick line corresponds to the true system $P(s)$. This figure gives an idea of the accuracy of the obtained initial model.

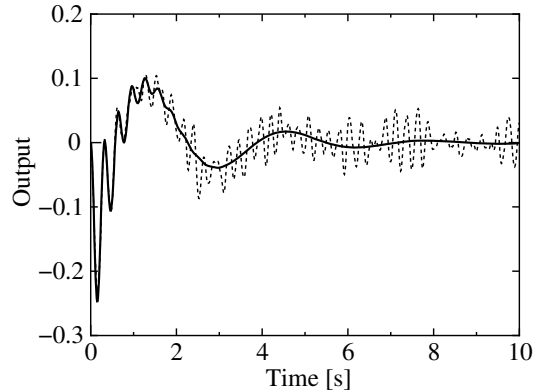


Fig. 1. An example of $\{g_i\}$ subject to colored noise.

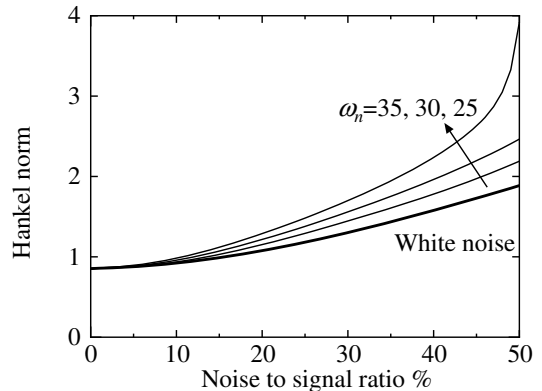


Fig. 2. $\|P(s) - \hat{P}(s)\|_H$ for various NSR (0 ~ 50%)

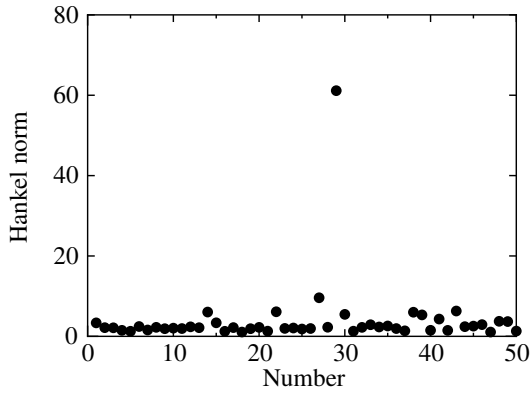


Fig. 3. $\|P(s) - \hat{P}(s)\|_H$ for 50 runs

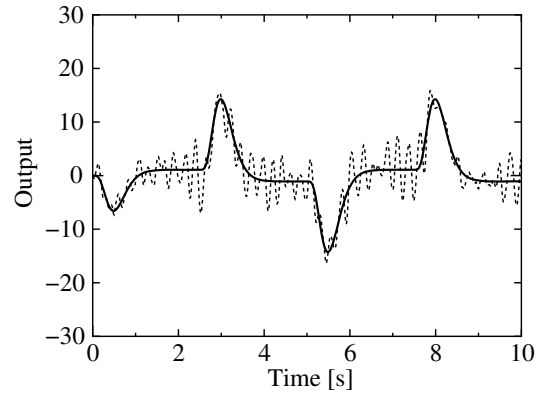


Fig. 5. Measured output $\tilde{y}^{10}(t)$ and its target $B^{10}(p)r(t)$

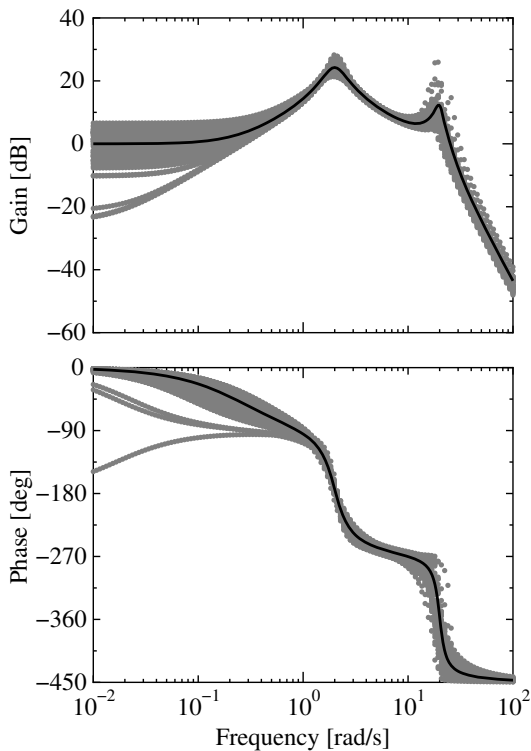


Fig. 4. Bode plots of initial estimate $\hat{P}(s)$

6.2 Convergence of iterative procedure

Next, we evaluate the convergence property for given \hat{M} . We add the colored measurement noise ($\omega_n = 25[\text{rad/s}]$ with NSR 50%) during the whole iteration as well. An example of the output $\tilde{y}^k(t)$ and its tracking reference $B^k(p)r(t)$ at $k = 10$ is shown in Fig. 5. The dotted line represents the output with noise and the thick line is the tracking reference. Since the measurement noise is so big, it is difficult to see the real tracking performance. Therefore, the true output (without noise) is shown in Fig. 6 with its tracking reference. These figures tell us that the tracking is almost achieved at 10-th iteration in spite of the heavy noise shown in Fig. 5. Since the tracking error information plays a crucial role in most ILC, this robustness (against the measurement noise) is outstanding from the viewpoint of ILC. Fig. 7 shows the behavior of the estimated parameters along the iteration number k . From

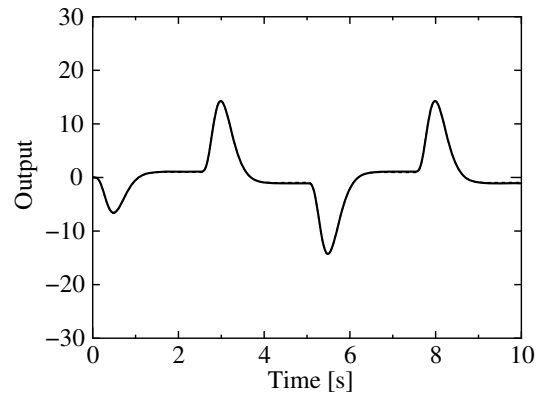


Fig. 6. True output $y^{10}(t)$ and its target $B^{10}(p)r(t)$

this figure, we see that each parameter approaches its true value quite quickly and smoothly. Within a few trial, the accuracy of the estimated model becomes satisfactory. We run the simulation 50 times (with different random noises), and Bode plots of the estimated models at $k = 10$ are shown in Fig. 8. Though it includes 50 lines, the deviation is so small. This figure also ensures us that we can obtain accurate models in the presence of both heavy colored noise and initial modeling errors.

Furthermore, we have run the simulation at NSR 100% with different types of colored noises. In total, we have 1,000 initial models, among which there exist 28 unstable models. However, the iterative identification procedure converges in **all** cases. This fact exhibits the robustness of the ILC based identification clearly.

7. CONCLUSION

This paper described a novel approach for identification of continuous-time systems based on ILC concepts. The method enable us to obtain an accurate model in the presence of heavy measurement noise through iterative learning control concepts. The robustness against noise is achieved through (i) projection of continuous-time I/O signals onto an appropriate finite dimensional parameter space, and (ii) noise tolerant learning laws. The robustness of the method against the heavy and colored measurement noise has been evaluated through extensive simulation study. In particular, (a) the accuracy of the initial models obtained through the preliminary experiments and (b) convergence property of the iterative learning against

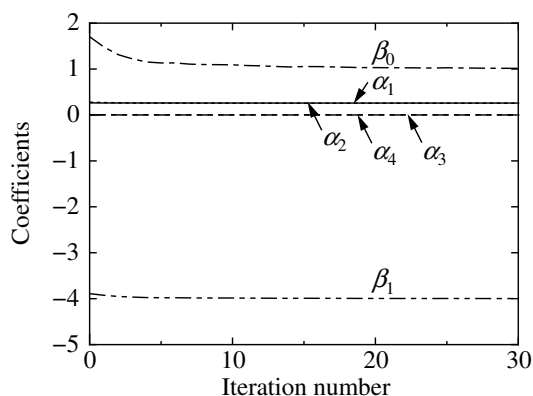


Fig. 7. Estimated system parameters at each iteration

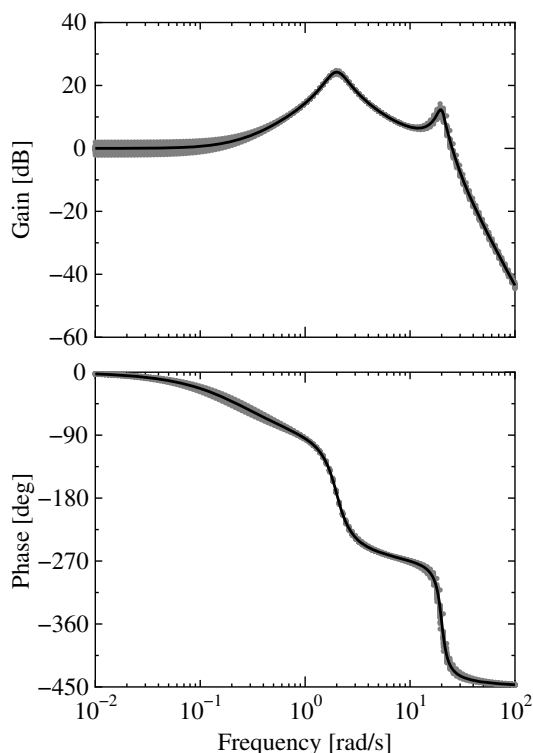


Fig. 8. Bode plots of 50 identified systems ($k = 10$)

errors in initial models are examined in the presence of various colored measurement noise. The effectiveness of the method has been demonstrated through numerical examples for a non-minimum phase system.

ACKNOWLEDGEMENTS

This paper is based on the joint work with Prof. Marco Campi. The authors would like to thank him.

REFERENCES

S. Arimoto, S. Kawamura, and F. Miyazaki. Bettering operation of robotics. *Journal of Robotic System*, 1(2): 123–140, 1984.

Z. Bein and J. X. Xu. *Iterative learning control – Analysis, design, integration and applications*. Kluwer Academic Press, Boston, 1998.

M. C. Campi, T. Sugie, and F. Sakai. Iterative identification method for linear continuous-time systems. In *Proc.*

of the 45th IEEE Conference on Decision and Control, pages 817–822, 2006.

Y. Chen and C. Wen. *Iterative learning control: convergence, robustness and applications*, volume LNCIS-248. Springer-Verlag, 1999.

H. Garnier and M. Mensler. The CONTSID toolbox: a matlab toolbox for CONTinuous-Time System Identification. In *Proc. of the 12th IFAC Symposium on System Identification, CD-ROM*, 2000.

H. Garnier and M. Mensler. CONTSID: a CONTinuous-Time System Identification toolbox for matlab. In *Proc. of the 5th European Control Conference*, 1999.

H. Garnier, M. Gilson, and E. Husestein. Developments for the Matlab CONTSID toolbox. In *Proc. of the 13th IFAC Symposium on System Identification, CD-ROM*, 2003.

K. Hamamoto and T. Sugie. An iterative learning control algorithm within prescribed input-output subspace. *Automatica*, 37(11):1803–1809, 2001.

K. Hamamoto and T. Sugie. Iterative learning control for robot manipulators using the finite dimensional input subspace. *IEEE Trans. Robotics and Automation*, 18(4):632–635, 2002.

S. Kawamura, F. Miyazaki, and S. Arimoto. Realization of robot motion based on a learning method. *IEEE Trans. on Systems, Man and Cybernetics*, 18(1):126–134, 1988.

K. L. Moore. *Iterative learning control for deterministic systems*, volume Springer-Verlag Series on Advances in Industrial Control. Springer-Verlag, London, 1993.

F. Sakai and T. Sugie. \mathcal{H}^2 -suboptimal iterative learning control for continuous-time system identification. In *Proc. of American Control Conference*, pages 946–951, 2006.

F. Sakai and T. Sugie. A continuous-time closed-loop identification based on iterative learning control concepts. In *Proc. of the 46th IEEE Conference on Decision and Control, (to appear)*, 2007.

N. K. Sinha and G. P. Rao. *Identification of Continuous-Time Systems*. Kluwer Academic Publishers, Dordrecht, 1991.

T. Sugie and T. Ono. An iterative learning control law for dynamical systems. *Automatica*, 27(4):729–732, 1991.

T. Sugie and F. Sakai. Noise tolerant iterative learning control for continuous-time systems identification. In *Proc. of the 44th IEEE Conference on Decision and Control and European Control Conference ECC 2005*, pages 4251–4256, 2005.

H. Unbehauen and G. P. Rao. Continuous-time approaches to system identification - a survey. *Automatica*, 26(1): 23–35, 1990.

P. Young. Parameter estimation for continuous-time models - a survey. *Automatica*, 17(1):23–39, 1981.